Available online at www.sciencedirect.com
ScienceDirect
Thin Solid Films 516 (2008) 2762–2766
www.elsevier.com/locate/tsf

Observation of negative differential resistance and single-electron tunneling in electromigrated break junctions

Yutaka Noguchi [a,*], Rieko Ueda [a], Tohru Kubota [a], Toshiya Kamikado [a], Shiyoshi Yokoyama [a], Takashi Nagase [b]

[a] Kobe Advanced ICT Research Center, National Institute of Information and Communications Technology, 588-2 Iwaoka, Nishi-ku, Kobe 651-2492, Japan
[b] Osaka Prefecture University, 1-1 Gakuen-cho, Nakaku, Sakai, Osaka 599-8531, Japan

Available online 5 May 2007

Abstract

We observed a negative differential resistance (NDR) along with single-electron tunneling (SET) in the electron transport of electromigrated break junctions with metal-free tetraphenylporphyrin (H_2BSTBPP) at a temperature of 11 K. The NDR strongly depended on the applied gate voltages, and appeared only in the electron tunneling region of the Coulomb diamond. We could explain the mechanism of this new type of electron transport by a model assuming a molecular Coulomb island and local density of states of the source and the drain electrodes.

PACS: 73.21.La; 73.23.Hk; 73.40.Rw
Keywords: Negative differential resistance; Single-electron tunneling; Single molecule transistor; Electromigration; Porphyrin

1. Introduction

Electron transport mechanisms in a nanoscale molecular junction, that is a single or a few molecules contacted by electrodes, has been widely investigated, because of their potential applications in nanometer-scale electronic systems [1,2]. In recent years, remarkable findings of these studies were made in observation of electron transport in single-molecule transistors (SMTs), which is a single-molecule in the middle of a nanogap electrode with a back gate structure, fabricated using an electromigration method [3–5]. Many groups have been reported that the electron transport in the SMTs is strongly affected by discrete energy states formed in the molecular system, as a result of the molecule in the junctions worked as a Coulomb island.

However, molecular deposition at nanogap electrodes of the SMTs is a random process and the mechanisms have not been fully clarified. Lack of a method for molecular deposition causes intrinsic difficulties in understanding electron transport properties in this system, because the electron transport in the molecular junction is very sensitive to atomic scale structural differences and surroundings of the molecule [6]. In addition, impurities such as unintended Au nano particles formed in the nanogaps acting like molecules in the SMTs were recently reported [7,8]. These facts suggest that the properties of the electromigrated break junction itself have not been fully understood.

We have been investigating the functions of porphyrin molecules as a nanoscale electronic element in multilayer tunneling junctions and nano-gap electrodes, and have shown that the molecules could work as a Coulomb island of these junctions [9,10]. In the present study, we report a new type of the electron transport property, i.e., the coexistence of single-electron tunneling (SET) and negative differential resistance (NDR), occurred in the electromigrated break junctions with 5,15-bis(3,5-di-t-butylphenyl)-10,20-bis(4-mercaptophenyl) porphyrin (H_2BSTBPP) at 11 K. We explained the mechanism of the electron transport in the junction by a model assuming a molecular Coulomb island and a local density of states (LDOS) of the source and the drain electrodes.

2. Experimental

Fig. 1a shows the sample structure and the experimental setup. An Au continuous lead (length: 150 nm, width: 80 nm,

* Corresponding author. Present address: Center of Frontier Science, Chiba University, 1-33, Yayoicho, Inageku, Chibashi, Chiba 263-8522 Japan.
E-mail address: y-noguchi@faculty.chiba-u.jp (Y. Noguchi).

0040-6090/$ - see front matter © 2007 Elsevier B.V. All rights reserved.
doi:10.1016/j.tsf.2007.04.111

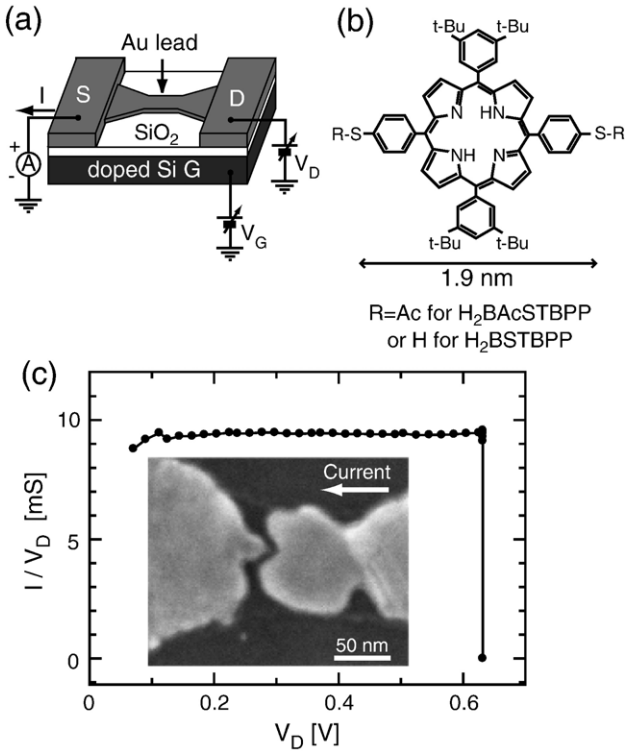

Fig. 1. (a) Schematic illustration of the sample structure and the experimental setup. (b) Chemical structure of H_2BAcSTBPP and H_2BSTBPP. (c) Typical conductance curve of the junction during the electromigration process. The inset shows a scanning electron micrograph of the junction after the breaking procedure.

thickness: 15 nm) and the pad electrodes with 2 nm thick Ti adherent layer were fabricated on a doped Si substrate with 50 nm thick SiO_2 using a combination of electron beam and photo lithography and a liftoff process.

Fig. 1b shows the chemical structure of H_2BSTBPP and its acetyl protected form (H_2BAcSTBPP). The acetyl protected thiol group prevents the molecule from forming S–S linkage in a solution phase. We prepared a 0.5 mM solution of H_2 BAcSTBPP in tetrahydrofuran (THF), and deprotected the molecule by adding 10 μL of NH_4OH to 4 mL of the solution 10 min before the self-assembly of H_2BSTBPP [11]. The substrate, after being cleaned with acetone, ethanol, and oxygen plasma, was immersed in the resulting solution at room temperature for 18 h. After the H_2BSTBPP assembled, the substrates were rinsed with THF and ethanol and finally N_2 blow-dried. These molecular deposition procedures were performed in oxygen-free conditions.

The samples were then transferred to a low temperature vacuum probe station. The electromigration process to form a break junction in the Au lead was performed at room temperature. Fig. 1c shows a typical conductance curve during the electromigration process. A ramp bias voltage was applied to the Au lead at a rate of 20 mV/s until the current dropped as a result of forming the break junction. The inset of Fig. 1c shows a scanning electron micrograph of the typical electromigrated break junction. We could obtain nanogap electrodes with a very narrow gap width, e.g., ≤5 nm. The details of the electromigration process have been reported in elsewhere [10,12]. The sample was then cooled to 11 K, and the current–voltage (I–V_D) curves were measured within the bias $|V_D| \leq 1$ V as a function of gate voltage (V_G).

3. Results and discussion

3.1. Statistics of the device fabrication

We measured the I–V curves of 141 junctions with H_2 BSTBPP and of 168 junctions with no molecules as a control experiment. Here, the control samples were prepared by just immersing bare-junctions in pure THF. The magnitude of the current observed in the junctions with no molecules tends to be lower than that of the junctions with H_2BSTBPP. We found the current lower than 1 pA at $V_D = 1$ V in 82 junctions with H_2 BSTBPP (58.1%), and in 133 junctions with no molecules (81.6%). In these insulating junctions, we can assume that the gap width was too large for the electron tunneling and no conductive materials existed in the middle of the nanogaps. The difference in the occurrence rate of the insulating junctions suggests that the conductance of the electromigrated break junctions was increased by the presence of H_2BSTBPP.

On the other hand, the microscopic differences in the structure of the nanogaps, e.g., morphology of the electrode surface, molecule/electrode contact, molecular order, and so on, cause a variety of I–V curves of the junctions. We previously reported typical I–V curves and their occurrence rate observed in the electromigrated break junctions with and without molecules [12].

In this study, we found the I–V_D curves indicating a direct tunneling between the nanogap electrode in 29 junctions with H_2BSTBPP (20.5%), and in 13 junctions with no molecules (8.0%), respectively. The electron transport mechanism in most of these junctions was attributed to the Fowler–Nordheim tunneling [12]. The I–V_D curves with a staircase behavior were observed in 30 junctions with H_2BSTBPP (21.3%), and the electron transport in 2 of these junctions could attribute to the SET from their V_G dependence. In other words, these 2 junctions, a candidate of the SMT, showed a Coulomb diamond in the dI/dV_D plot vs. V_G and V_D (the differential conductance map). On the other hand, no gate-dependent I–V_D curves were found in the junctions with no molecules, although 17 junctions (10.4%) showed a staircase behavior. While the Coulomb diamond was observed in a few junctions, we were able to obtain data suggesting a successful fabrication of SMT. The data show a new type of electron transport in the electromigrated break junctions, i.e., the gate-dependent NDR along with SET.

3.2. Gate-dependent NDR

We firstly show the gate-dependent NDR without SET observed in the junction with H_2BSTBPP. Fig. 2a is the differential conductance map. The NDR regions are indicated by broken lines. Fig. 2b shows the I–V_D curves at $V_G = -1.5$, -3.0, and -4.5 V. One can see that the NDR appears at both

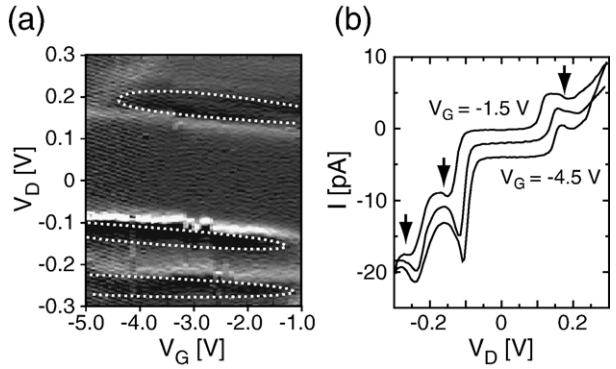

Fig. 2. (a) Differential conductance map of the H_2BSTBPP junction. The gate-dependent NDR is shown. The conductance range is from −0.05 nS (black) to 0.5 nS (white). White broken lines indicate the NDR regions. V_D occurring the NDR shifts proportionally as a function of V_G. (b) Selected I–V_D curves of the junction at V_G=−1.5, −3.0, and −4.5 V. The arrows indicate the positions of NDR. For clarify, the curves are shifted vertically.

positive and negative bias, and the bias voltages occurring the NDR proportionally shift as a function of V_G. Many researchers have found molecular contributions to NDR in atomic scale tunneling junctions using a scanning tunneling microscope [13–15], in molecular junctions using a nanometer-scale device [16], and in electromigrated break junctions [17]. Although various mechanisms of the NDR have been proposed, taking into account the V_D and V_G dependence and the asymmetric I–V_D curves, the one that appeared in our experiment is most likely to electron transport involving discrete states in the electronic structure.

We propose a model to explain a possible mechanism of the gate-dependent NDR (Fig. 3). The model is consisting of a source electrode (S), an LDOS of the source (s-LDOS), an LDOS of the drain (d-LDOS), a drain electrode (D), and a gate electrode (not appeared in the illustrations). The model assumes that the s-LDOS and d-LDOS are caused by adsorbates. The adsorbates should have a capacitive coupling with the source or drain, and gate electrodes. Although the origin of the adsorbates causing the LDOSs have not been identified, H_2BSTBPP is a possible candidate in our junctions. Some molecules in the air, such as H_2O or O_2, are also likely to be the origin of the adsorbate, because a similar type of the gate-dependent NDR in the electromigrated break junctions with no molecules have been reported by the other research group [17].

Fig. 3 represent schematic energy diagrams of the junction. The applied V_G proportionally shift the potential of the LDOS due to a finite capacitance formed between the adsorbate and the gate electrode (see top schematics in Fig. 3). Thus the V_D giving the NDR also depends on the V_G (middle and bottom schematics in Fig. 3). Here, the top schematics of Fig. 3 are the energy diagram at V_D=0 V, and middle and bottom schematics are the one appearing the current peak at positive V_D, and at negative V_D, respectively. As shown in these figures, the both peaks appeared at positive and negative V_D shift with a same slope by applying V_G. The model can reasonably explain the characteristics of the gate-dependent NDR shown in Fig. 2.

3.3. Negative differential resistance along with SET

Fig. 4a is a differential conductance map of the junction showing the NDR along with SET. A corresponding map of the conductance features is also shown for clarification. A Coulomb diamond due to the SET appears in Fig. 4a, and it is closed at a voltage V_G=4.6 V. The dI/dV_D –V_G plots at V_D=0 V is shown in Fig. 4b for clarification. One can see the conductance peak of a Coulomb oscillation at V_G=4.6 V. A resonance due to tunneling into an excited state with energy about 40 meV above the ground states of the Coulomb island is indicated by an arrow in Fig. 4a.

The excited state appeared in Fig. 4a may be due to the molecular vibrational mode of H_2BSTBPP [3,18]. Measurements of resonance Raman spectra of metal-free tetraphenylporphine (H_2-TPP) have indicated that a very strong band exists at a frequency of 334 cm^{-1} (41.4 meV) attributed to the porphyrin skeletal vibration of H_2-TPP [19]. This value agrees well with that obtained in our experiment. We have not observed such states in the control samples and in the junctions with other molecules.

Interestingly, the NDR depending on the V_G was observed along with the Coulomb diamond in the junction (Fig. 4a). The NDR regions are indicated by broken lines in Fig. 4a, and the I–V_D curves at V_G=1.5, 3.0, 4.5, and 6.0 V are also shown for clarification (Fig. 4c). The NDR regions are seen at both the positive and the negative V_D, and proportionally shift as a function of V_G. However, the slopes of the NDR appeared in positive and negative V_D region is different, while that is independent of the bias polarity in Fig. 2a.

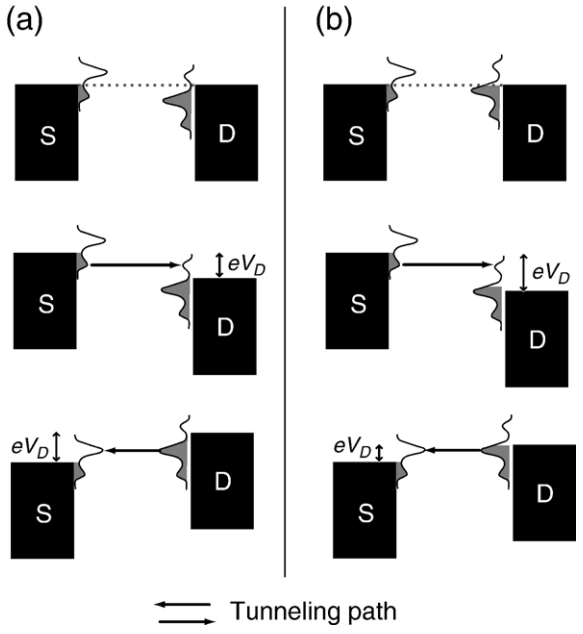

Fig. 3. Schematic energy diagrams of S/s-LDOS/d-LDOS/D junction. The applied V_G for (a) is larger than that for (b). Top schematics are the energy diagram at V_D=0 V. Middle and Bottom schematics are the one when the current peak appears at positive and negative V_D, respectively. One can see the NDR shift proportionally as a function of V_G.

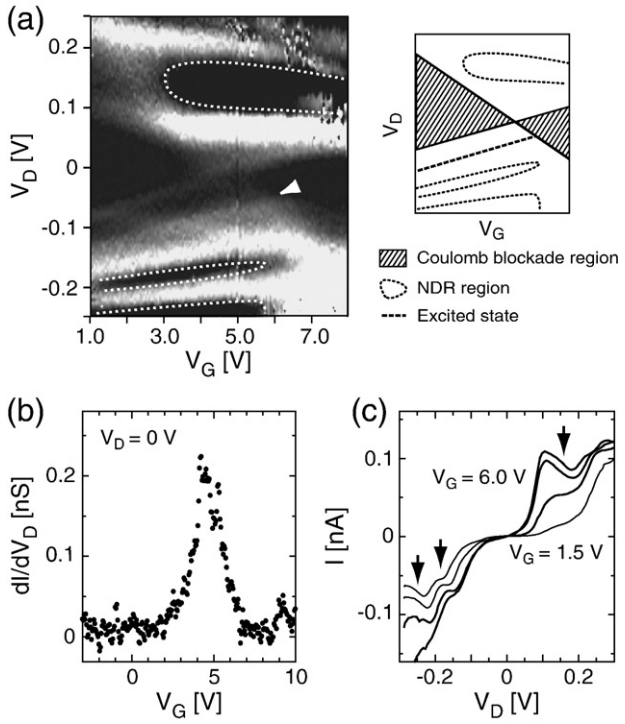

Fig. 4. (a) Differential conductance map of the H_2BSTBPP junction (left). The gate-dependent NDR with SET is shown. The conductance range is from −0.05 nS (black) to 1 nS (white). A corresponding map of these conductance features is also shown for clarification (right). (b) dI/dV_D − V_G plots at V_D=0 V. A peak of Coulomb oscillation appears at V_G=4.6 V. (c) Selected I–V_D curves of the H_2BSTBPP junction at V_G=1.5, 3.0, 4.5, and 6.0 V. The arrows indicate the positions of NDR.

A possible explanation of the multiple different slopes in the differential conductance map is that a device possessing parallel multiple current paths with the different sets of capacitances. However, in Fig. 4a, the NDR appears only in the electron tunneling region (not appear in the blockaded region), and the conductance peaks are strongly enhanced in that region. These mean that the multiple slopes are not independent of each other and the NDR should occur due to the electron tunneling involving the Coulomb island. Thus we believe that a series model rather than a parallel one is better to explain the electron transport mechanism of the junction. Moreover, we found the electron transport properties can be well described by using the model shown in Fig. 3 with assuming a molecular Coulomb island (Fig. 5).

The model is based on the Coulomb blockade theory in the molecular system [3,4,20]. The μ_n shown in Fig. 5a is the electrochemical potential defined as the additional energy of the n-th electron to the Coulomb island including the chemical potential and Coulomb blockade energy. The excited state due to the molecular vibration is located ΔE above the μ_n. The μ_S and μ_D correspond to the work functions of the source and the drain electrode, respectively.

Fig. 5a, b, and c represents the possible energy diagrams of the junction corresponding to applied gate voltages of 4.6, 6.0, and 3.2 V in Fig. 4a, respectively. Fig. 5a shows the condition when the Coulomb diamond is closed. The vibration-assisted tunneling occurs when both μ_n and the excited state are located between μ_S and μ_D (Fig. 5b bottom). When the peak of s-LDOS and μ_S align with μ_n, increasing the applied V_D clearly causes NDR (Fig. 5c middle and bottom). Because the potential of s-LDOS is also varied by applying V_G as the μ_n, the relative potential difference of these two states is unlikely to change (see at V_D=0 V in Fig. 5a, b, and c). This causes the weak V_G dependence of the NDR, consequently the multiple different slopes that appeared at positive V_D as shown in Fig. 4a. On the other hand, the NDR that appeared at negative V_D depends on V_G almost the same as the slope of Coulomb diamond due to the strong coupling of the d-LDOS with the drain electrode.

The model can explain the gate-dependent NDR along with SET appeared in our junction by assuming the molecular Coulomb island that possessing discrete energy states. In addition, the mechanism of the multiple different slopes of the gate-dependent NDR can be also described by this model. We note here that discrete energy states in the Coulomb island are required to explain the NDR along with SET. This means that a molecule rather than the unintended metallic particles formed during the electromigration process [7,8] is likely to be the Coulomb island of the junction. We thus believe that the H_2 BSTBPP was working as a Coulomb island of the junction.

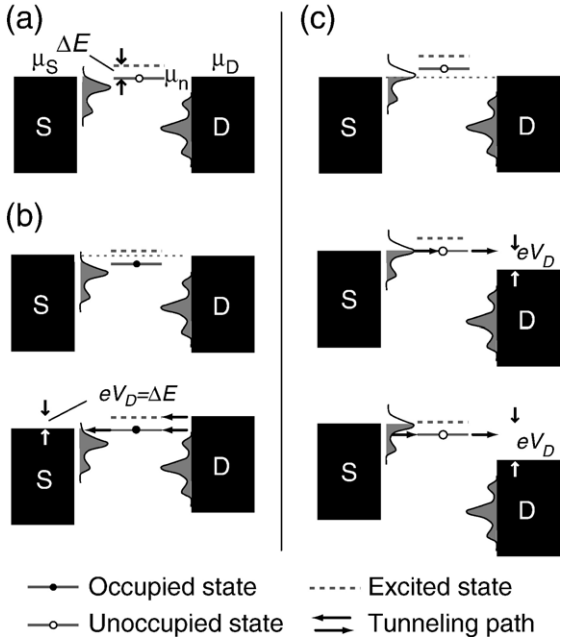

Fig. 5. Schematic energy diagrams of S/s-LDOS/a molecular Coulomb island/d-LDOS/D junction. (a), (b), and (c) represent the possible energy diagrams corresponding to applied gate biases V_G of 4.6, 6.0, and 3.2 V in Fig. 2(a), respectively. Electron transport is allowed when μ_n is located between μ_S and μ_D. (a) μ_n aligns with μ_S and μ_D (V_D=0 V), meaning that the Coulomb diamond is closed. (b) Top schematic is the energy diagram at V_D=0 V. Bottom schematic is the one when μ_n and μ_D aligns with μ_S and the excited state, respectively. eV_D is equal to the energy of vibrational mode (ΔE). (c) Top schematic is the energy diagram at V_D=0 V. Middle schematic is the one when s-LDOS peak aligns with μ_n and μ_S. Bottom schematic is the one when NDR is occurring. s-LDOS contributing to the current is decreasing with increasing V_D.

4. Conclusion

We have measured the I–V_D curves of 141 electromigrated break junctions with H_2BSTBPP and 168 junctions without molecules at a temperature of 11 K. We observed a new type of electron transport, i.e., NDR along with SET, in the junction with H_2BSTBPP. The excited state located 40 meV above the ground state possibly due to the porphyrin skeletal vibration was also observed in the junction. The model assuming a molecular Coulomb island and the LDOS of the source and the drain electrodes could well describe this new type of electron transport properties of the junction.

Acknowledgements

This work was partly supported by a Grant-in-Aid for Scientific Research from the Ministry of Education, Culture, Sports, Science and Technology and by the Hyogo Science and Technology Association.

References

[1] A. Nitzan, M.A. Ratner, Science 300 (2003) 1384.
[2] C. Joachim, M.A. Ratner, Proc. Natl. Acad. Sci. 102 (2005) 8801.
[3] H. Park, J. Park, A.K.L. Lim, E.H. Anderson, A.P. Alivisatos, P.L. McEuen, Nature 407 (2000) 57.
[4] J. Park, A.N. Pasupathy, J.I. Goldsmith, C. Chang, Y. Yaish, J.R. Petta, H. D. Abruna, M. Rinkoski, J.P. Sethna, H.D. Abruna, P.L. McEuen, D.C. Ralph, Nature 417 (2002) 722.
[5] W. Liang, M.P. Shores, M. Bockrath, J.R. Long, H. Park, Nature 417 (2002) 725.
[6] Y. Noguchi, M. Iwamoto, T. Kubota, S. Mashiko, IEICE Trans. E85-C (2002) 1247.
[7] R. Sordan, K. Balasubramanian, M. Burghard, K. Kern, Appl. Phys. Lett. 87 (2005) 013106-1.
[8] A.A. Houck, J. Labaziewicz, E.K. Chan, J.A. Folk, I.L. Chuang, Nano Lett. 5 (2005) 1685.
[9] Y. Wakayama, K. Ogawa, T. Kubota, H. Suzuki, T. Kamikado, S. Mashiko, Appl. Phys. Lett. 85 (2004) 329.
[10] Y. Noguchi, T. Nagase, T. Kubota, T. Kamikado, S. Mashiko, Thin Solid Films 499 (2006) 90.
[11] F.-R.F. Fan, Y. Yao, L. Cai, L. Cheng, J.M. Tour, A.J. Bard, J. Am. Chem. Soc. 126 (2004) 4035.
[12] Y. Noguchi, T. Nagase, R. Ueda, T. Kamikado, S. Kubota, S. Mashiko, Jpn. J. Appl. Phys. 46 (2007) 2683.
[13] Y. Xue, S. Datta, S. Hong, R. Reifenberger, J.I. Henderson, C.P. Kubiak, Phys. Rev., B 59 (1999) R7852.
[14] J. Gaudioso, L.J. Lauhon, W. Ho, Phys. Rev. Lett. 85 (2000) 1918.
[15] C. Zeng, H. Wang, B. Wang, J. Yang, J.G. Hou, Appl. Phys. Lett. 77 (2000) 3595.
[16] J. Chen, W. Wang, M.A. Reed, A.M. Rawlett, D.W. Price, J.M. Tour, Appl. Phys. Lett. 77 (2000) 1224.
[17] L.H. Yu, D. Natelson, Nanotechnology 15 (2004) S517.
[18] A.N. Pasupathy, J. Park, C. Cheng, A.V. Soldatov, S. Lebedkin, R.C. Bialczak, J.E. Grose, L.A.K. Donev, J.P. Sethna, D.C. Ralph, P.L. McEuen, Nano Lett. 5 (2005) 203.
[19] P. Stein, A. Ulman, T.G. Spiro, J. Phys. Chem. 88 (1984) 396.
[20] D.L. Klein, R. Roth, A.K.L. Lim, A.P. Alivisatos, P.L. McEuen, Nature 389 (1997) 699.